

THE INFLUENCE OF AG DOPING ON STRUCTURAL AND ELECTRICAL RESISTIVITY PROPERTIES OF $Y_3Ba_5Cu_{8-x}Ag_xO_{18-\delta}$ HIGH TEMPERATURE SUPERCONDUCTING ALLOYS

Puwanasingam, M., P.R. Fernando*, and F.C. Ragel
Department of Physics, Eastern University, Sri Lanka

ABSTRACT

This research paper describes the synthesis of a series of Y-based superconducting alloys doped with Ag oxide. The $Y_3Ba_5Cu_{8-x}Ag_xO_{18-\delta}$ superconducting alloys were synthesized by Gholipour et al. (2012), Tavana et al. (2010) and Khosroabadi et al. (2014) using sol-gel reaction technique. In the present research $Y_3Ba_5Cu_{8-x}Ag_xO_{18-\delta}$ superconducting alloys were synthesized by solid state reaction technique. These alloys were investigated by using X-ray diffraction pattern (XRD), Scanning Electron Microscope (SEM) image and the electrical resistivity, ρ , measurements. The ρ measurements above room temperature of Y358 alloys shows metal behavior in the normal state. The YBCO alloy family was exposed having the CuO_2 planes and the Cu-O chains. Increasing the number of the CuO_2 planes and the position of the Cu-O chains have positive effects on the significance of the transition temperature in the Y-based alloys. The X-ray diffraction patterns were accepted by Joint Committee of Powder Diffraction Standards (JCPDD) database software, which the Ag ions substitute in symmetrical phase of the alloy. The replacement of the Ag ions in the CuO_2 plane of symmetric phase has been associated with the Ag ions in the Y123 alloys, which replace in the Cu-O chain. The ρ of these alloys were measured employing four-probe point technique and the $\rho(T)$ curves agreed the transition temperature develops above 100 K.

Keywords: Four-probe point technique, transition temperature, silver, Y358, Y123, X-ray diffraction pattern, Scanning Electron Microscope image, electrical resistivity, metal behavior.

*Corresponding author: rodneypaper@gmail.com



<https://orcid.org/0000-0003-3698-3347>

1.0 INTRODUCTION

In 1987, Chu and co-workers [1] found the first high temperature superconductors in $\text{YBa}_2\text{Cu}_3\text{O}_7$ (Y123) alloy showed the superconducting transition temperature (T_c) at 92 K. The research was continued for $\text{YBa}_2\text{Cu}_4\text{O}_8$ (Y124) and $\text{Y}_2\text{Ba}_4\text{Cu}_7\text{O}_{15}$ (Y247) alloys and found that these alloys showed superconducting transition temperatures (T_c) at 80 K [2] and 40 K [3], respectively. Recently, a new $\text{Y}_3\text{Ba}_5\text{Cu}_8\text{O}_{18}$ (Y358) high-temperature superconductor was introduced by Taviana [4] and Aliabadi *et al.* [5] which exhibits superconducting above 100 K. The change in the superconducting transition temperatures depends on the number of CuO_2 planes and CuO chain in the crystal structures. The $\text{YBa}_2\text{Cu}_3\text{O}_7$ superconductor consists 2 CuO_2 planes and a CuO chain. The $\text{YBa}_2\text{Cu}_4\text{O}_8$ superconductor consists a CuO double chain [4, 5]. The $\text{Y}_2\text{Ba}_4\text{Cu}_7\text{O}_{15}$ superconductor consists a CuO_2 plane and a CuO chain, and a double chain. $\text{Y}_3\text{Ba}_5\text{Cu}_8\text{O}_{18}$ superconductor consists a crystalline structure, which is similar to $\text{YBa}_2\text{Cu}_3\text{O}_7$ superconductor with 5 CuO_2 planes and 3 CuO chains [4, 5]. The highest number of CuO_2 planes and CuO chains play an important role on in T_c of Y358 [4, 5].

The transition temperature of the YBCO superconducting alloys was improved by doping with other group elements such as Ag and Cu. Wu *et al.* [1] investigated Y123 superconductor with transition temperature about 90 K has one CuO chain and two CuO_2 planes. Gholipour *et al.* [6], Taviana *et al.* [4] and Khosroabadi *et al.* [7] studies reveal that the Y358 superconducting alloys have transition temperature in the range of 101 to 110 K with the Ag doping. The variation in the transition temperature is due to the presence of various crystal structures presents in the Y358 superconducting alloys. The crystal structure Pmmm2 which consists five CuO_2 planes and three CuO chains and lattice parameter a, b and c are 3.845 Å, 3.894 Å and 31.093 Å respectively Gholipour *et al.* [6]. The other crystal structure pmmm that consists six CuO_2 planes and two CuO chains and lattice parameter a, b and c are 3.838 Å, 3.904 Å and 31.043 Å respectively [4-6].

Doping the YBCO superconducting alloys with Ag doping will be the enrichment of the critical current density, inter atomic bonds between the grains, improves the grain growth and crystal orientations [7,8]. Therefore, doping Y358 superconducting alloys with Ag will modify the superconducting properties.

The aim of this research is to study the effect on structural and electrical properties of the $Y_3Ba_5Cu_{8-x}Ag_xO_{18-\delta}$ superconducting alloys synthesized by solid-state reaction technique. The characterization of the alloys has been analyzed by using X-ray diffraction (XRD), Scanning Electron Microscope (SEM) images with energy dispersive x-rays (EDX) and the four-probe technique.

2.0 EXPERIMENTAL METHODOLOGY

The $Y_3Ba_5Cu_{8-x}Ag_xO_{18}$ ($x = 0.1, 0.2$ and 0.3) superconducting alloys were prepared by using standard solid-state reaction technique and labeled as sample1, sample2 and sample3. The oxide powers of high purity (99.99 %) (Alfa Aesar) Yttrium Oxide(Y_2O_3), Copper (ii) Oxide(CuO), Barium Carbonate($BaCO_3$), and Silver Oxide(Ag_2O), were used as starting materials. Weighted dry powders were grounded and mixed by using an agate mortar and pestle until the colour of the mixture becomes dark and to form a good homogeneity. After that, the mixture was calcined in an alumina crucible at a constant temperature $900\text{ }^\circ\text{C}$ for 24 hours in a controlled oxygen atmosphere with a specific thermal program to remove the unwanted oxides and carbonates. Then the calcined mixture was allowed to slowly furnace cooled to room temperature in air (the cooling rate was maintained $100\text{ }^\circ\text{C}$ per hour until $400\text{ }^\circ\text{C}$ and $200\text{ }^\circ\text{C}$ per hour from $400\text{ }^\circ\text{C}$ down to room temperature). After that the calcined mixture was reground and three sets of pellet of diameter of 14 mm and thickness 1-2 mm were prepared under the applied pressure of 300 kg.cm^{-2} by employed dry pressing. This process was repeated three times at a constant temperature $950\text{ }^\circ\text{C}$ for 24 hours and the pallets were thoroughly reground and pelletized to 300 kg.cm^{-2} in each sintering. Then the pallets were re-grounded once more and then final powder samples were compacted in the form of pellets under the applied pressure 340 kg.cm^{-2} . Finally, the pellets were sintered in the furnace at $940\text{ }^\circ\text{C}$ for 24 hours and left in the furnace to cool down to room temperature.

The crystal structure, phase and lattice spacing of the alloys were obtained by conventional symmetrical θ - 2θ x-ray diffraction using Rigaku Ultima IV X-Ray system available at University of Sri Jayawadanapura, Sri Lanka. The Rigaku Ultima IV X-Ray system is set-up in the Bragg-Brentano geometry. In order to ensure that only the sample was radiated, 0.5° anti-scatter slit with a 10 mm mask was also used in the incident beam path. No further slits were used in the path of the diffracted beam. Wide angle 2θ scans in the range of 10° to 100° with a step

stage of 0.02° , with the Cu tube at a generated voltage of 40 kV and current of 40 mA was used. All XRD experiments were performed at room temperature. The $\text{CuK}\alpha$ radiation was in part removed, by adding a Ni filter in front of the detector. In order to determine if an alloy button is single-phase or multi-phase, the phases were identified by comparing the measured XRD patterns to that in the Joint Committee of Powder Diffraction Standards (JCPDD) database.

The Zeiss EVO 15LS scanning electron microscope (SEM) was used to investigate the actual chemical composition and surface morphology of the alloys, available at University of Peradeniya, Sri Lanka. The sample disc was mounted in a Cu holder and a carbon tape was used for connectivity between the sample disc and the Cu holder. Dust particles that can contaminate the sample disc was removed using compressed air before loading it inside the microprobe chamber. In order to do the spot analyses on an alloy, initially an area on the alloy was magnified to $50\ \mu\text{m}$. In the selected alloy area, ten light and dark spots were selected, in five different regions. From this data, the average compositions of the individual elements at these spots were calculated. Finally, the alloy's surface morphology was analyzed using the scanning electron microscope option of the EMPA.

The electrical resistivity measurements were done in the temperature range from 77 K to 153 K by using standard four-probe resistance measurement equipment.

3.0 RESULT AND DISCUSSION

XRD Measurement

Figure 1 shows the X-ray diffraction peaks for $\text{Y}_3\text{Ba}_5\text{Cu}_{8-x}\text{Ag}_x\text{O}_{18-\delta}$ ceramic alloys ($x = 0.1, 0.2$ and 0.3) were collected at room temperature in the 2θ range from 10° to 90° . These peaks were obtained using Rigaku Ultima IV X-Ray Diffractometer with $\text{Cu-K}\alpha$ radiation and crystal graphical computer aid program was used to analyses the crystal structure. The main peaks in all samples belong to the Y358/Ag alloys. The lattice parameters did not depart from the orthorhombic cell, thus indicating that Ag atoms do not disturb the orthorhombic structure of $\text{Y}_3\text{Ba}_5\text{Cu}_{8-x}\text{Ag}_x\text{O}_{18-\delta}$ ceramic alloys. As we expect, twin peaks at 46.70 and 47.32 indicate the presence of orthorhombic structure in the $\text{Y}_3\text{Ba}_5\text{Cu}_{8-x}\text{Ag}_x\text{O}_{18-\delta}$ ($x = 0.1, 0.2$ and 0.3) ceramic alloys.

Although, all the alloys clearly evident the presence of Ag atoms in a metal phase at the peak position $2\theta = 38.225^\circ$. However, the intensity of the Ag peak decreases with increasing the Ag concentration. Moreover, less dominant impurity phases can be observed in the alloy systems. Although, when the Ag substitution increases, the lattice positions of occupancy number Cu (1) become less. The designated Miller indices and volume fraction phase is 83 % of pmmm structure.

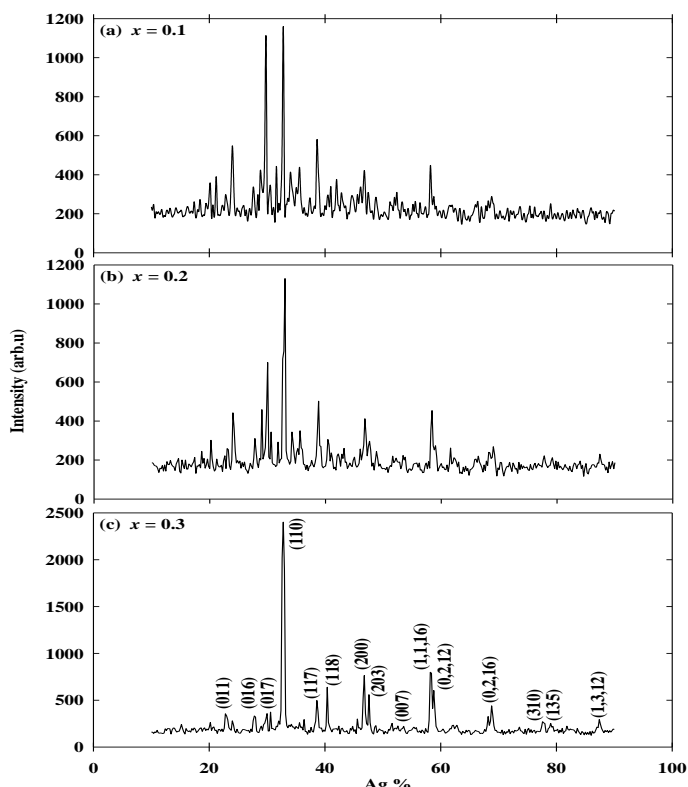


Figure 1: The X-ray diffraction peaks for $Y_3Ba_5Cu_{8-x}Ag_xO_{18-\delta}$ ceramic alloys with Ag concentration (a) $x = 0.10$, (b) $x = 0.20$ and (c) $x = 0.30$.

The change in the lattice parameters a and c are shown in Figure 2 and unit cell volume, V and the density, d , are shown in Figure 3. The data in Figure 2 clearly indicates that a increases and c decreases linearly with increasing the Ag concentration, within a very small limit of $a \approx 0.04 \text{ \AA}$ and $c \approx 0.258 \text{ \AA}$. This indicates that the Ag substitution don't not change the orthorhombic crystal structure of the ceramic superconductors, as well as the doublets at 46.92° and 47.51° indicates the presence of orthorhombic crystal structure [9]. The decrease in c is due to the presence of (007) peak in Y235 superconductors [10].

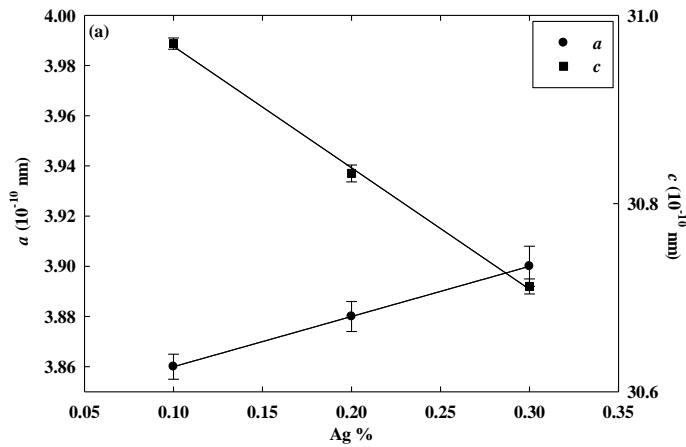


Figure 2: The change in lattice parameters a and c as a function of Ag %.

In Figure 3, the variation in the unit cell volume shows a parabolic behavior while the density decreases with increasing the Ag concentration. However, the variation is not considerably a large deviation. The variation in these physical parameters indicates that the Cu^{2+} atoms of atomic radius $r_{\text{Cu}^{2+}} = 0.72 \text{ \AA}$ [10-12] may be replaced by the Ag atoms of atomic radius, $r_{\text{Ag}^+} = 1.26 \text{ \AA}$ [10-12], which is in agreement with previous studies [13]. Moreover, another fact the Cu^{2+} atoms may be partly replaced by Ag^+ atoms [10-12]. Although, the slight increase in oxygen concentration could be change the physical properties of these superconductors. However, the values of a , b , V and d of these alloys are in agreement with literatures [14-20]; whereas c agrees with literatures [14-16].

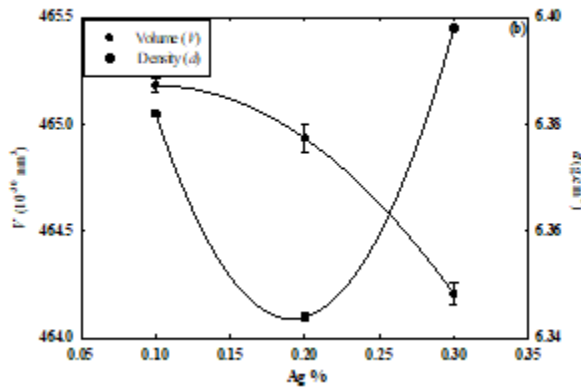


Figure 3: The change in the unit cell volume, V , and the density, d , as a function of Ag %.

Scanning Electron Microscope (SEM) Measurement

The chemical composition, surface morphology and the nature of grains were investigated using Scanning Electron Microscope. This produced high resolution images of sample surface tend to know the nature of grains and porous size. The Energy Dispersive X-ray (EDX) analysis used to investigate the actual chemical composition in the prepared ceramic alloys.

Figure 4 (a) to (c) show SEM micrographs as well as the EDX spectrum for the manufactured ceramic alloys.

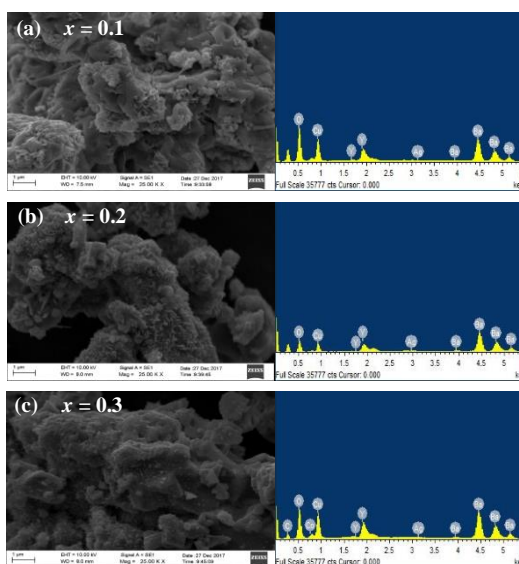


Figure 4: The SEM image and the EDX spectrum of $Y_3Ba_5Cu_{8-x}Ag_xO_{18-\delta}$ alloys with (a) $x = 0.1$, (b) $x = 0.2$ and (c) $x = 0.3$.

All the alloys show crystalline homogeneous coral reef like structure with pores between the grains. The surface morphology shows that these alloys have strong bonds between the grains, which is in agreements with the results of X-ray peaks, density of the alloys and the electrical resistivity. The presence of pores can be reduced by the changing the palletization pressure, annealing and sintering temperature and time [10]. Grain size increase with increasing the Ag concentration, indicates that the Cu^{2+} ions are substituted by the Ag^+ ions [17]. The EDX analysis were carried out in the showed surface area that clearly shows the presence of all the ions in the Y358 superconducting alloys. The nominal and the average (Avg.) actual atomic concentration obtained from the electron

microprobe of alloys with standard deviation (Std. Dev) are tabulated in Table 1, which shows a slight variation between nominal and actual compositions obtained from the EDX. The slight change may be due to the loss of chemical during manufacturing or evaporation. It is supervised that the Ag peak height is very small comparing with then other ions. This may be the fact that the Ag well mixed in the alloy system [10]. However, the presence of Ag in the alloys system can be confirmed by the increasing behavior of the grain size [10].

Electrical Resistivity Measurement

Electrical resistivity, ρ , as a function of temperature, T , in the temperature range from 80 to 160 K was measured using four probe technique, while cooling and heating. Figures 5 (a), (b) and (c) curves only represents the measurement during cooling up to 160 K. There is no any observed hysteresis behavior in the process of heating and cooling the alloys. All the alloys show a metallic behavior above its onset superconducting transition temperature, $T_{C(\text{onset})}$. This behavior is due to the bosons and fermion are limited to the CuO plans, thus by scattering of the bosons from the fermions to forms the ρ in the plans [21] and exclude the electron-phonon interaction due to very small electron-phonon coupling constant [22]. A small arc in the $\rho(T)$ curves are observed just below the superconducting transition temperature, $T_{C(\text{onset})}$, indicates thermodynamic fluctuations in the alloys system.

Table 1: The nominal and the average (Avg.) actual atomic concentration obtained from the electron microprobe of alloys with standard deviation (Std. Dev).

Nominal Concentration	Y (at. %)		B (at. %)		Cu (at. %)		Ag (at. %)		O (at. %)	
	Avg.	Std.Dev	Avg.	Std.Dev	Avg.	Std.Dev	Avg.	Std.Dev	Avg.	Std.Dev
$Y_2Ba_2Cu_{7.5}Ag_{0.1}O_{18-5}$	3.02	± 0.01	4.98	± 0.02	7.85	± 0.01	0.09	± 0.01	84.60	± 0.04
$Y_2Ba_2Cu_{7.2}Ag_{0.2}O_{18-5}$	2.98	± 0.01	4.92	± 0.03	7.80	± 0.03	0.18	± 0.01	84.12	± 0.02
$Y_2Ba_2Cu_{7.7}Ag_{0.2}O_{18-5}$	2.92	± 0.03	4.88	± 0.01	7.65	± 0.01	0.32	± 0.00	84.23	± 0.01

These thermodynamic fluctuations arises at a finite series below $T_{C(\text{onset})}$, due to the presence of cooper pairs [23]. A single sharp superconducting transition can be seen in the alloys expose the formation of single Y358/Ag phase. The sharp transition is due to the good couplings between the grains, which can be confirmed from the surface morphology from SEM images as well as good crystallinity, and higher value of Orth. F. from the XRD measurements [24].

The superconducting transition temperature, $T_{C(\text{onset})}$ was calculated from the intersect point of the gradient as indicated by dashed lines in each panel are guides to the eye, zero transition temperature $T_{C(\text{offset})}$, and superconducting temperature T_{SC} as well as the transition width $\Delta T_C = T_{C(\text{onset})} - T_{C(\text{offset})}$, are tabulated in Table 2.

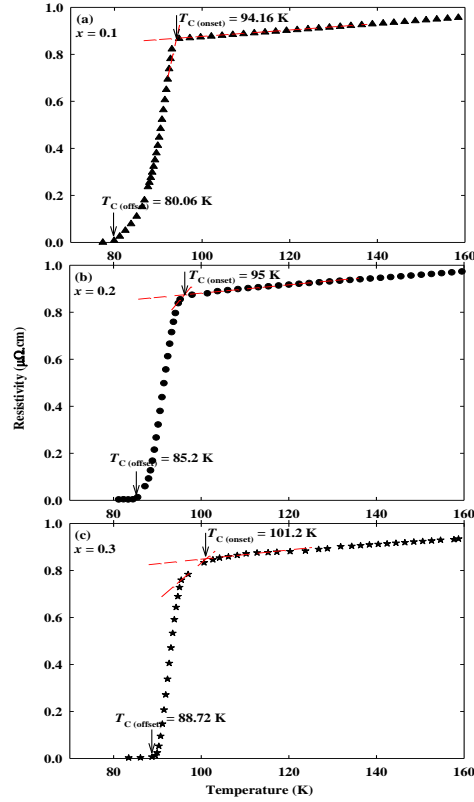


Figure 5: The normalized electrical resistivity ρ , as a function of temperature, T for the $\text{Y}_3\text{Ba}_5\text{Cu}_{8-x}\text{Ag}_x\text{O}_{18-\delta}$ alloys with nominal concentrations (a) $x = 0.10$, (b) $x = 0.20$ and (c) $x = 0.30$ in the range $80 \text{ K} \leq T \leq 160 \text{ K}$. The dashed lines in each panel are guides to the eye as to indicate the transitions in the $\rho(T)$ curve when the alloy is cooled from the metallic region, through the superconducting transition region. $T_{C(\text{onset})}$, $T_{C(\text{offset})}$ and T_{SC} are onset, zero and superconducting transition temperatures respectively.

The alloys show T_{SC} at 86.75 K, 90.10 K and 94.96 K for concentrations 0.1, 0.2 and 0.3 respectively, which deviates the results reported by Zarabina *et al.* [9]. In the present work, the variation in the $T_{C(\text{onset})}$, $T_{C(\text{offset})}$ and T_{SC} may be depends on

the manufacturing technique and processes, sintering temperature, pelletizing pressure and calcinations and sintering time. However, these transition temperatures increase with increasing the Ag % which reveals that the Ag atoms influence the Y358 alloys system.

The broadening in the transition width ΔT_C may be the effect of the survival of impurity phases and low electrical conductivity between the grains, causes by low sintering temperature [23]. Moreover, manufacturing method, calcinations duration, sintering time and temperature are the external factors and the development of phase in the grain boundaries are the internal factors influence the ΔT_C [23].

Table 2: The transition temperatures and ΔT_C of the $Y_3Ba_5Cu_{8-x}Ag_xO_{18-\delta}$ alloys.

Sample	T_c (onset) K	T_c (offset) K	T_{SC}	K ΔT
$Y_3Ba_5Cu_{7.9}Ag_{0.1}O_{18-\delta}$	94.16	80.06	86.75	11.70
$Y_3Ba_5Cu_{7.8}Ag_{0.2}O_{18-\delta}$	95.00	85.20	90.10	8.00
$Y_3Ba_5Cu_{7.7}Ag_{0.3}O_{18-\delta}$	101.2	88.72	94.96	11.88

4.0 CONCLUSION

In the present study, the influences of Ag atoms to the high temperature superconductor $Y_3Ba_5Cu_{8-x}Ag_xO_{18-\delta}$ with nominal concertation ($x = 0.1, 0.2$ and 0.3) were investigated by X-ray diffraction (XRD), scanning electron microscope (SEM) with Energy dispersive X-rays (EDX) and four-point electrical resistivity probe measurements.

The X-ray diffraction peaks were indicating that Ag doping atoms do not affect the orthorhombicity of $Y_3Ba_5Cu_8O_{18-\delta}$ compound. The intensity of the Ag peak decreases with increasing the Ag concentration.

From SEM analysis, all the alloys show crystalline homogeneous coral reef like structure with pores between the grains and the surface morphology, shows that these alloys have strong bonds between the grains, which is in agreements with the results of X-ray peaks, density of the alloys and the electrical resistivity. The

EDX analysis were carried out in the showed surface area that clearly shows the presence of all the ions in the Y358 superconducting alloys.

The resistivity versus temperature curves were shown that the transition temperatures were changed, that the value of transition temperatures was increased with addition of Ag atoms ($x = 0.1, 0.2$ and 0.3) which reveals that the Ag atoms influence the Y358 alloys system. The superconductor ceramic alloys have superconducting transition temperatures at 86.75 K, 90.10 K and 94.96 K for concentrations 0.1, 0.2 and 0.3 respectively.

Therefore, that the Ag atoms were affect the $Y_3Ba_5Cu_8O_{18-\delta}$ alloy systems and the transition temperature of the Y358 alloys system increases with increasing the Ag concentration without changing its orthorhombic structure.

References

- [1] Wu, K., Ashburn, J. R., Torng, C. J., Hor, P. H., Meng, R. L., Gao, L., Huang, Z. J., Wang, Y. Q., and Chu, C. W (1987). *Phys. Rev. Lett.* 58: 908.
- [2] Marsh, P., Fleming, R. M., Mandich, M. L., De Santolo, A. M., Kwo, J., Hong, M., and Martinez-Miranda, L.J. (1988). *Nature*, 334: 660
- [3] Bordet, P., Chaillout, C., Chenavas, J., Hodeau, J. L., Marezio, M., Karpinski, J., and Kaldis, E. (1988). *Nature* 336: 596.
- [4] Tavana, A., and Akhavan, M. (2010). *The European Physical Journal B* 73: 79-83.
- [5] Aliabadi, A., Farshchi, Y. A., and Akhavan, M. (2009). *Physica C* 469: 2012–2014.
- [6] Gholipour, S., Daadmehr, V., Rezakhani, A. T., Khosroabadi, H., Shahbaz Tehrani, F., and Hosseini Akbarnejad, R. (2012). *Journal of Superconductivity and Novel Magnetism* 25: 2253-2258.
- [7] Khosroabadi, H., Rasti, M., and Akhavan, M. (2014). *Physica C* 497: 84–88.

- [8] Tepea, M., Avcia, I., Kocoglua, H., and Abukayb, D. (2004). *Solid State Communications* 131: 319–323.
- [9] Zarabinia, N., Daadmeh, r V., Shahbaz, Tehrani, F., and Abbasi, M. (2015). *Procedia Materials Science*. 11: 242-247.
- [10] Aylin, Y., Kemal, K., and Gonul, B. A. (2012). 25: 1459-1467.
- [11] Behera, D., Mishra, N. C., and Patnaik, K. (1997). *J. Supercond.* 10(1): 27-32.
- [12] Taylor, C. R., and Greaves, C. (1994). *Physica C* 235: 853-864.
- [13] Azambuja, P., Júnior, P. R., Jurelo, A. R., Serbena, F. C., Foerster, C. E., Costa, R. M., Souza, G. B., Lepienski, C. M., and Chinelatto, A. L. (2009). *Braz. J. Phys.* 39(4): 638-644.
- [14] Gholipour, S., Daadmehr, V., Rezakhani, A. T., Khosroabadi, H., Shahbaz, F. T., and Hosseini, R. A. (2012). *J. Supercond Nov Magn.* 25: 2253-2258.
- [15] Aliabadi, A., Farshchi, Y. A., and Akhavan, M. (2009). *Physica C* 469: 2012-14.
- [16] Tavana, A., and Akhavan, M. (2010). *Eur Phys. J. B* 73: 79-83.
- [17] Udomsamuthirun, P., Kruaehong, T., Nikamjon, T., and Ratreng, S. (2010). *J. Supercond. Nov. Magn.* 23: 1377.
- [18] Topal, U., Akdogan, M., and Ozkan, H. (2011). *J. Supercond. Nov. Magn.* 11: 1176-1182.
- [19] Topal, U., and Akdogan, M. (2011). *J. Supercond. Nov. Magn.* 11: 1285-1287.
- [20] Ayas, A. O., Ekicibil, A., Cetin, S. K., Coskun, A., Er A. O., Ufuktepe, Y., Firat, T., and K1ymac, K. (2011). *J. Supercond. Nov. Magn.* 11: 1192-1199.

- [21] Martin, S., Fiory A. T., Fleming, R. M., Schneemeyer, L. F., and Waszczak, J. V. (1990). *Physical Review B*, 41(1): 846-849.
- [22] Anderson, P. W., and Zou Z. (1988). *Physical Review Letters*, 60(2): 132-135.
- [23] Nayera, H. M., Ramadan, A., Abou-Aly, A., Ibrahim, H. I., and Mohammed, S. H. (2012). *Materials Sciences and Applications*, 3: 224-233.
- [24] Mustafa, M. D., Abdul H. S., Hussein B., Naif M. Al-Hada., Chen S. K., Rabaah S. A., Mohd M. A. K., Zainal A. T., and Roslan A. S. (2017). *Results in Physics*, 7: 407-412.